Available online at www.sciencedirect.com
ScienceDirect
European Journal of Medicinal Chemistry 44 (2009) 1180–1187
EUROPEAN JOURNAL OF MEDICINAL CHEMISTRY
http://www.elsevier.com/locate/ejmech

Original article

Predicting anti-HIV activity of 1,3,4-thiazolidinone derivatives: 3D-QSAR approach

V. Ravichandran [a], B.R. Prashantha Kumar [b], S. Sankar [b], R.K. Agrawal [a,*]

[a] *Pharmaceutical Chemistry Research Laboratory, Department of Pharmaceutical Sciences, Dr. H.S. Gour Vishwavidyalaya, Sagar 470 003, MP, India*
[b] *Department of Pharmaceutical Chemistry, J.S.S. College of Pharmacy, Ooty, TN, India*

Received 8 February 2008; received in revised form 11 April 2008; accepted 22 May 2008
Available online 12 June 2008

Abstract

HIV-1 (human immunodeficiency virus type-1) is the pathogenic retrovirus and causative agent of AIDS. HIV-1 RT is one of the key enzymes in the duplication of HIV-1. Inhibitors of HIV-1 RT are classified as NNRTIs and NRTIs. NNRTIs bind to a region that is not associated with the active site of the enzyme. Within the NNRTIs category, there is a set of inhibitors commonly referred to as thiazolidinone derivatives. The present 3D-QSAR study attempts to explore the structural requirements of thiazolidinone derivatives for anti-HIV activity. Based on the structures and biodata of previous thiazolidinone analogs, 3D-QSAR studies have been performed with a training set consisting of 96 molecules, which resulted in two reliable computational models, CoMFA and CoMSIA with r^2 values of 0.931 and 0.972, standard error of estimation (SEE) of 0.173 and 0.089, and q^2 values of 0.663 and 0.784, respectively, with the number of partial least-squares (PLS) components being six. It is shown that the steric and electrostatic properties predicted by CoMFA contours and the hydrogen bond acceptor, hydrogen bond donor, and hydrophobic properties predicted by CoMSIA contours are related to anti-HIV activity. The predictive ability of the resultant model was evaluated using a test set comprising of 17 molecules and the predicted r^2 values of CoMFA and CoMSIA models were 0.861 and 0.958, respectively. These models are more significant guide to trace the features that really matter especially with respect to the design of novel compounds.

Keywords: Anti-HIV; 3D-QSAR; CoMFA; CoMSIA; Thiazolidinone

1. Introduction

HIV-1 (human immunodeficiency virus type-1) is the pathogenic retrovirus and causative agent of AIDS or AIDS-related complex (ARC) [1,2]. When a viral RNA is translated into a polypeptide sequence, it is assembled in a long polypeptide chain, which includes several individual proteins namely, reverse transcriptase, protease, integrase, etc. Before these enzymes become functional, they must be cut from the longer polypeptide chain.

Acquired immune deficiency syndrome (AIDS) is a formidable pandemic that is still wreaking havoc world wide. The catastrophic potential of this virally caused disease may not have been fully realized. The causative moiety of the disease is human immunodeficiency virus (HIV), which is a retrovirus of the lentivirus family [3]. The three viral enzymes namely reverse transcriptase, protease and integrase encoded by the *gag* and *gag–pol* genes of HIV play an important role in the virus replication cycle. Among them, viral reverse transcriptase (RT) catalyzes the formation of proviral DNA from viral RNA, the key stage in viral replication. Its central role in viral replication makes RT a prime target for anti-HIV therapy [4].

Computational chemistry has developed into an important contributor towards rational drug design. Quantitative structure–activity relationship (QSAR) modeling results in a quantitative correlation between chemical structure and biological activity. QSAR analyses of HIV-1 reverse transcriptase inhibitors [5,6], HIV-1 protease inhibitors [7–10], HIV-1

* Corresponding author. Tel.: +91 7582 265457; fax: +91 7582 264236.
E-mail addresses: dragrawal2001@yahoo.co.in, phravi75@rediffmail.com (R.K. Agrawal).

0223-5234/$ - see front matter © 2008 Elsevier Masson SAS. All rights reserved.
doi:10.1016/j.ejmech.2008.05.036

integrase inhibitors [11,12] and gp 120 envelope glycoprotein [13] were reported. Leonard and Roy have reported a few QSAR models for anti-HIV activities of different groups of compounds [14,15]. The present group of authors have reported a few quantitative structure–activity relationship models to predict the anti-HIV activity of different groups of compounds [16–23]. In continuation of such efforts, in this article, we have performed 3D-QSAR analysis to explore the correlation between physicochemical properties and anti-HIV-l activity of thiazolidinone derivatives and established two 3D-QSAR models, CoMFA and CoMSIA to guide further structural optimization and predict the potency and physicochemical properties of clinical drug candidates (Fig. 1).

In the present work we have taken 113 compounds and their anti-HIV activities from the reported work [24–29]. Anti-HIV activity of all 113 compounds was determined in the same laboratory using same procedure even though the compounds have been synthesized by different group of authors. There is high structural diversity and a sufficient range of biological activity in the selected series of compounds. This insists to select these series of compounds for our 3D-QSAR study. All the anti-HIV activities used in the present study were expressed as $pEC_{50} = -\log_{10} EC_{50}$, where EC_{50} is the micro molar concentration of the compounds producing 50% reduction in the cytopathic effect caused by the virus which is stated as the means of at least two experiments. EC_{50} values were assessed by XTT assays [30]. The compounds which were not showing confirmed anti-HIV activity in the above-cited literature have not been taken for our study.

2. Materials and methods

CoMFA and CoMSIA are powerful and established tools for building 3D-QSAR models that can be applied to drug design [31,32]. Consequently, we used the structures of 113 (96 compounds in training set and 17 compounds in test set) thiazolidinone analogs (Table 1) and their anti-HIV activities (EC_{50} in μM) in MT-4 cells to establish and validate CoMFA and CoMSIA models in the present study. Three-dimensional structure building and all the modeling were carried out using the SYBYL 6.7 (sgi work station) program package and conformations of compounds in the training and test sets were generated using the systematic conformational search method implemented in SYBYL 6.7 [33]. Energy minimization was

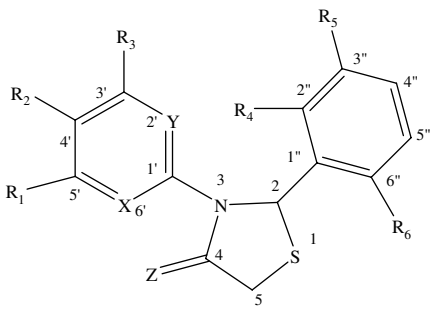

Fig. 1. Basic structure of thiazolidinone analogs.

effected using the Tripos force field with a distance-dependent dielectric and the Powell conjugate gradient algorithm with a convergence criterion of 0.001 kcal/mol. Partial atomic charges were calculated using Gasteiger–Huckel method [34].

Cross-validated q^2 usually serves as the quantitative measurement for the robustness of CoMFA and CoMSIA. Necessity of a good alignment is a basic requirement of the COMFA procedure, as designed by Cramers at TRIPOS C. Alex Tropsha also underlines the necessity for a good alignment [35]. Consequently, the thiazolidinone compounds were aligned according to their common substructure-compound **68** (Table 1), one of the most promising analogs in the inhibition of HIV-1 (III_B) replication in MT-4 cells. The optimal number of components obtained is then used to derive the final QSAR model using all the compounds (without cross-validation). The conventional r^2 is used to measure the quality of the model.

The total set of compounds was initially divided randomly into two groups as training and test sets, having 96 compounds in training set and 17 compounds in the test set. Test and training set compounds were chosen manually such that low, moderate and high activity compounds were present approximately in equal proportions in both sets. Training set compounds were used to develop the CoMFA and CoMSIA models and the test set compounds were used to validate the developed model. Group cross-validation (5 groups) and scrambling of the biological data (randomization control) were performed to test the stability and reliability of the models.

2.1. CoMFA models

We have tried molecular fit, atom fit and field fit alignment methods but molecular alignment was effected with the 'field fit alignment method' (Fig. 2). After consistently aligning the molecules within the lattice that extended 4 Å units beyond the aligned molecules in all directions with a grid step size of 2 Å, a probe sp^3 carbon atom with +1 net charge and Van der Waals radius of 1.52 Å were employed. 3D-QSAR models were built by field fit alignment method in SYBYL. Steric and electrostatic interactions between the probe and the remaining molecules were calculated. The generated steric and electrostatic fields were scaled by the CoMFA-STD method in SYBYL 6.7 with a default energy of 30 kcal/mol. Electrostatic interactions were modeled using a Coulomb potential and Van der Waals interactions using a Lennard–Jones potential. The regression analysis was carried out using the partial least-squares (PLS) method and cross-validation was performed using leave-one-out method with 2 kcal/mol column filter. The final model was developed with an optimum number of components yielding the highest q^2.

2.2. CoMSIA models

Method proposed by Klebe and coworkers [36], with the same lattice box as that used for the CoMFA calculations, was followed to derive CoMSIA. Five physicochemical properties, such as steric, electrostatic, hydrophobic, hydrogen

Table 1
Structures of thiazolidinone derivatives

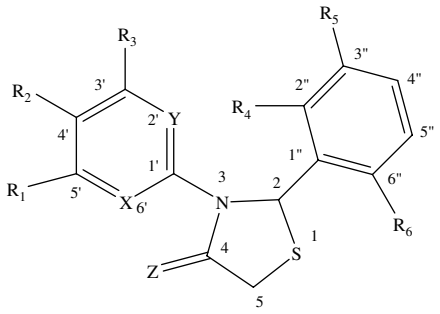

Compound no.	X	Y	Z	R_1	R_2	R_3	R_4	R_5	R_6
1	N	N	O	H	H	H	Cl	H	Cl
2	N	N	O	H	H	H	Cl	H	F
3	N	N	O	H	H	Me	Cl	H	F
4	N	N	O	H	H	Me	Cl	H	Cl
5	N	N	O	H	H	Me	F	H	F
6	N	N	O	Me	H	Me	Cl	H	F
7	N	N	O	Cl	H	Me	Cl	H	Cl
8	N	N	O	Me	H	Me	Cl	H	Cl
9	N	N	O	Me	H	Me	F	H	F
10	N	N	O	OMe	H	Me	Cl	H	F
11	N	N	O	OMe	H	Me	Cl	H	Cl
12	N	N	O	OMe	H	Me	F	H	F
13	N	N	O	Me	H	CF_3	Cl	H	Cl
14	N	N	O	OH	H	Me	Cl	H	Cl
15	N	N	O	Me	H	CF_3	Cl	H	F
16	N	N	O	Me	H	Ph	Cl	H	Cl
17	N	N	O	Me	H	CF_3	F	H	F
18	N	N	O	Me	H	Ph	Cl	H	F
19	N	N	O	Me	H	Ph	F	H	F
20	N	N	O	Me	Me	Me	F	H	F
21	N	N	O	Me	Me	Me	Cl	H	Cl
22	N	N	O	Me	Me	Me	Cl	H	F
23	Pyrimidin-4-yl		O	2,6-Dimethyl			Cl	H	Cl
24	Pyrimidin-4-yl		O	2,6-Dimethyl			Cl	H	F
25	Pyrimidin-4-yl		O	2,6-Dimethyl			F	H	F
26	CH	CH	O	H	H	Me	F	H	OMe
27	CH	CH	O	H	H	Me	Cl	Me	F
28	CH	CH	O	H	H	Me	OMe	H	OMe
29	N	CH	O	Me	H	H	F	H	OMe
30	N	CH	O	Me	H	H	Me	H	Me
31	N	CH	O	Me	H	H	F	H	CF_3
32	N	CH	O	Me	H	H	Cl	H	F
33	N	CH	O	Me	H	H	OMe	H	OMe
34	N	CH	O	H	H	Me	Me	H	Me
35	N	CH	O	H	H	Me	F	H	OMe
36	N	CH	O	H	H	Me	F	H	CF_3
37	N	CH	O	H	H	Me	Cl	H	F
38	N	CH	O	H	H	Me	OMe	H	OMe
39	N	CH	O	H	H	Br	Me	H	Me
40	N	CH	O	H	H	Br	F	H	CF_3
41	N	CH	O	H	H	Br	F	H	OMe
42	N	CH	O	H	H	Br	Cl	H	F
43	N	CH	O	H	H	Br	OMe	H	OMe
44	N	CH	O	Me	H	Me	Me	H	Me
45	N	CH	O	Me	H	Me	F	H	OMe
46	N	CH	O	Me	H	Me	F	H	CF_3
47	N	CH	O	Me	H	Me	Cl	H	F
48	N	CH	O	Me	H	Me	OMe	H	OMe
49	N	N	O	H	H	Me	Me	H	Me
50	N	N	O	H	H	Me	F	H	OMe
51	N	N	O	H	H	Me	F	H	CF_3

Table 1 (*continued*)

Compound no.	X	Y	Z	R_1	R_2	R_3	R_4	R_5	R_6
52	N	N	O	H	H	Me	Cl	H	F
53	N	N	O	H	H	Me	OMe	H	OMe
54	CH	CH	O	H	H	H	Cl	H	Cl
55	CH	CH	O	H	H	H	F	H	F
56	N	CH	O	H	H	H	Cl	H	Cl
57	N	CH	O	H	H	H	Cl	H	F
58	N	CH	O	H	H	H	F	H	F
59	N	CH	O	H	Cl	H	Cl	H	Cl
60	N	CH	O	H	Cl	H	Cl	H	F
61	Pyridin-3-yl		O	–	H	H	F	H	F
62	N	CH	O	H	Cl	H	F	H	F
63	N	CH	O	H	Br	H	Cl	H	Cl
64	N	CH	O	H	Br	H	Cl	H	F
65	N	CH	O	H	Br	H	F	H	F
66	N	CH	O	Br	H	H	Cl	H	Cl
67	N	CH	O	Br	H	H	Cl	H	F
68	N	CH	O	Br	H	H	F	H	F
69	N	CH	O	H	H	Me	Cl	H	Cl
70	N	CH	O	H	H	Me	Cl	H	F
71	3-Me-Pyridin-2-yl		O	H	H	H	F	H	F
72	N	CH	O	H	H	Me	F	H	F
73	N	CH	O	H	Me	H	Cl	H	Cl
74	N	CH	O	Me	H	H	Cl	H	Cl
75	N	CH	O	Me	H	H	Cl	H	F
76	N	CH	O	H	Me	H	F	H	F
77	N	CH	O	Me	H	H	F	H	F
78	N	CH	O	Me	H	Me	Cl	H	Cl
79	N	CH	O	Me	H	Me	Cl	H	F
80	N	CH	O	Me	H	Me	F	H	F
81	N	CH	S	Me	H	H	F	H	F
82	N	CH	S	H	H	Me	F	H	F
83	N	N	S	H	H	Me	Cl	H	Cl
84	N	CH	S	Me	H	H	Cl	H	Cl
85	N	H	S	Me	H	Me	F	H	F
86	N	H	S	Br	H	H	F	H	F
87	H	H	O	H	H	Br	Cl	H	Cl
88	H	H	O	H	H	Br	Cl	H	F
89	H	H	O	H	H	Br	F	H	F
90	H	H	O	H	H	Cl	Cl	H	Cl
91	H	H	O	H	H	Cl	Cl	H	F
92	H	H	O	H	H	Cl	F	H	F
93	H	H	O	H	H	Me	Cl	H	Cl
94	H	H	O	H	H	Me	Cl	H	F
95	H	H	O	H	H	Me	F	H	F
96	H	H	O	H	H	Et	Cl	H	Cl
97	H	H	O	H	H	Et	Cl	H	F
98	H	H	O	H	H	Et	F	H	F
99	H	H	O	H	H	OMe	Cl	H	Cl
100	H	H	O	H	H	OMe	Cl	H	F
101	H	H	O	H	H	NO_2	Cl	H	Cl
102	H	H	O	H	H	NO_2	Cl	H	F
103	H	H	O	H	H	OMe	F	H	F
104	H	H	O	H	H	NO_2	F	H	F
105	H	H	O	Cl	H	Cl	Cl	H	Cl
106	H	H	O	Cl	H	Cl	F	H	F
107	H	H	O	F	H	F	Cl	H	Cl
108	H	H	O	Cl	H	Cl	Cl	H	F
109	H	H	O	F	H	F	Cl	H	F
110	H	H	O	F	H	F	F	H	F
111	H	H	O	Me	H	Me	Cl	H	Cl
112	H	H	O	Me	H	Me	Cl	H	F
113	H	H	O	Me	H	Me	F	H	F

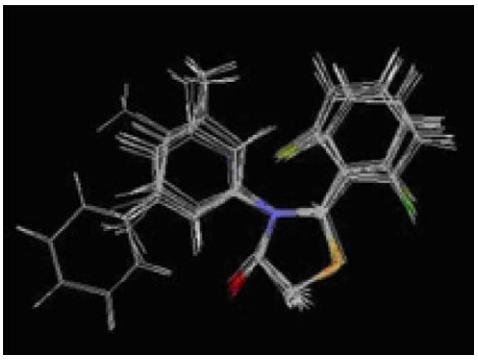

Fig. 2. Aligned thiazolidinone molecules by field fit alignment method.

bond donor, and hydrogen bond acceptor fields, were evaluated on the probe atom. Gaussian-type distance dependence was studied to measure the relative attenuation of the field position of each atom in the lattice. The use of Gaussian-type distance dependence in CoMSIA led to much smoother sampling of the fields around the molecules when compared to CoMFA. A default value of 0.3 was used as the attenuation factor.

In optimizing CoMSIA performance, the most important parameter is how to combine the five fields in a CoMSIA model. To choose the optimal result, we systemically altered the combination of fields and chose that value which gave the best non-cross-validation, smallest errors, and the largest F value. Finally, the model generated by combining the steric, electrostatic, hydrophobic, hydrogen bond donor and acceptor fields was selected as the best CoMSIA model, and the contours were analyzed using this model.

2.3. Regression analysis

To derive 3D-QSAR models, the CoMFA and CoMSIA descriptors were used as independent variables and the pEC_{50} activity value was used as a dependent variable. Partial least-squares (PLS) regression analyses were conducted with standard implementation in the SYBYL package. The predictive ability of the models was evaluated by leave-one-out (LOO) cross-validation. The cross-validated correlation coefficient, q^2, was calculated using Eq. (1).

$$r^2_{CV} = 1 - \frac{\sum_{i=1}^{N}\left(y_{exp} - y_{pred}\right)^2}{\sum_{i=1}^{N}\left(y_{exp} - y_m\right)} \quad (1)$$

$$PRESS = \sum_{i=1}^{N}\left(y_{exp} - y_{pred}\right)^2 \quad (2)$$

where y_{exp} is the activity for training set compounds, y_m is the mean observed value, corresponding to the mean of the values for each cross-validation group, and y_{pred} is the predicted activity for y_{exp}.

3. Results and discussion

We developed CoMFA model which is having both steric and electrostatic fields. The statistical parameters of the models are given in Table 2. The experimental and predicted activities are listed in Table 3. For the selected CoMFA model, the cross-validated r^2 (q^2) value of the training set was 0.663 with five principal components. The non-cross-validated r^2 value was 0.931 with standard error of estimation (SEE) 0.173 and covariance ratio (F) of 187.76 (significant at 99% level). Group cross-validation (5 groups) and scrambling of the biological data (randomization control) were performed to test the stability and reliability of the models. The average q^2 values obtained in the group cross-validation and randomization exercises are 0.630 and 0.143, respectively. The CoMFA model was externally validated with test set of compounds. The squared correlation coefficient (r^2 between EA and PA) value of validation set was 0.861 with standard error of estimation (SEE) 0.429. These results authenticate the good prediction ability of this 3D-QSAR model.

For the CoMSIA model, the cross-validated r^2 (q^2) value of the training set was 0.784 with six principal components. The non-cross-validated r^2 value was 0.972 with standard error of estimation (SEE) 0.089. The average q^2 values obtained in the group cross-validation and randomization exercises are 0.742 and 0.107, respectively. The CoMSIA model was externally

Table 2
PLS statistics of CoMFA and CoMSIA models

PLS statistics	CoMFA	CoMSIA							
	SE	SE	SHE	SED	SEA	SEHD	SEDA	SEHA	SEHDA
q^2	0.663	0.643	0.586	0.578	0.672	0.613	0.678	0.742	0.784
S_{PRESS}	0.784	0.712	1.016	1.370	0.983	1.271	1.225	0.533	0.456
R^2	0.931	0.926	0.910	0.899	0.928	0.916	0.964	0.970	0.972
S	0.173	0.232	0.287	0.375	0.226	0.262	0.202	0.113	0.089
F	187.76	166.12	156.88	120.11	168.20	163.12	188.93	210.17	212.85
Components	5	5	6	6	6	6	6	6	6
Steric	0.413	0.398	0.160	0.408	0.118	0.200	0.217	0.220	0.196
Electrostatic	0.587	0.602	0.572	0.514	0.473	0.480	0.430	0.358	0.360
Hydrophobic	–	–	0.268	–	–	0.275	–	0.110	0.120
H-acceptor	–	–	–	–	0.409	–	0.312	0.312	0.242
H-donor	–	–	–	0.088	–	0.045	0.41	–	0.082

S = steric field, E = electrostatic field, H = hydrophobic field, D = hydrogen bond donor, A = hydrogen bond acceptor.

Table 3
Experimental and predicted anti-HIV activities of thiazolidinone derivatives

Compound	CoMFA			CoMSIA	
	pEC_{50} (μM)	PA	Res.	PA	Res.
Training set					
1	0.644	0.834	−0.190	0.688	−0.044
2	0.236	0.499	−0.263	0.265	−0.029
3	1.131	1.001	0.130	1.162	−0.031
5	0.409	0.505	−0.096	0.507	−0.098
6	1.420	1.321	0.099	1.432	−0.012
9	0.767	0.754	0.013	0.965	−0.198
10	1.252	1.197	0.055	1.285	−0.033
12	0.578	0.561	0.017	0.576	0.002
13	0.000	0.181	−0.181	0.095	−0.095
15	−0.114	0.007	−0.121	−0.173	0.059
16	−0.785	−0.759	−0.026	−0.893	0.108
18	−0.591	−0.622	0.031	−0.584	−0.007
19	−0.806	−0.781	−0.025	−0.809	0.003
20	0.398	0.402	−0.004	0.403	−0.005
23	−0.634	−0.599	−0.034	−0.323	−0.311
24	−0.634	−0.711	0.078	−0.624	−0.010
25	−1.407	−1.407	0.000	−1.206	−0.201
26	−0.065	0.010	−0.074	−0.052	−0.013
27	−0.060	0.002	−0.062	−0.015	−0.045
28	−0.281	−0.250	−0.031	−0.270	−0.011
29	0.056	0.103	−0.047	0.103	−0.047
31	−0.326	−0.313	−0.013	−0.323	−0.003
32	0.492	0.536	−0.044	0.586	−0.094
33	−0.522	−0.420	−0.102	−0.624	0.102
34	−0.188	−0.159	−0.029	−0.187	−0.001
35	0.541	0.523	0.018	0.542	−0.001
36	−0.480	−0.493	0.013	−0.383	−0.097
37	−0.134	−0.155	.021	−0.147	0.014
39	−0.801	−0.773	−0.029	−0.797	−0.004
40	0.182	0.177	0.005	0.281	−0.099
42	0.457	0.429	0.029	0.448	0.009
43	1.347	1.383	−0.036	1.351	−0.004
44	−0.639	−0.647	0.008	−0.646	0.008
45	0.695	0.545	0.150	0.683	0.012
46	−0.769	−0.713	−0.057	−0.967	0.198
47	0.631	0.603	0.028	0.681	−0.050
48	−0.053	0.001	−0.055	0.004	−0.057
49	−0.533	−0.589	0.056	−0.529	−0.004
50	0.274	0.245	0.029	0.265	0.009
51	0.037	0.038	−0.001	0.037	0.000
52	0.114	0.224	−0.110	0.124	−0.010
53	0.043	0.034	0.010	0.043	0.000
54	0.397	0.367	0.030	0.297	0.100
55	−0.362	−0.321	−0.041	−0.351	−0.011
56	0.750	0.708	0.042	0.738	0.012
57	0.556	0.561	−0.005	0.566	−0.010
58	0.068	0.068	0.000	0.067	0.001
59	−0.250	−0.259	0.009	−0.251	0.001
60	−0.328	0.110	−0.439	−0.201	−0.127
62	−0.857	−0.839	−0.017	−0.854	−0.003
63	−0.179	−0.157	−0.022	−0.276	0.097
64	−0.093	−0.054	−0.039	−0.184	0.091
65	−0.686	−0.633	−0.053	−0.623	−0.063
66	0.565	0.611	−0.045	0.561	0.004
67	1.194	1.056	0.138	1.156	0.038
68	1.523	1.487	0.036	1.487	0.036
69	0.833	0.720	0.113	0.926	−0.093
70	1.004	0.981	0.023	1.102	−0.098
72	−0.395	−0.110	−0.284	−0.314	−0.081
73	−0.149	0.009	−0.158	−0.108	−0.041
74	1.357	1.292	0.065	1.299	0.058
75	1.276	0.950	0.325	1.235	0.041
77	1.086	0.480	0.606	1.018	0.068
78	1.046	0.775	0.271	1.126	−0.080
79	1.377	0.897	0.480	0.971	0.406
80	1.229	0.619	0.610	1.324	−0.095
81	−0.814	−0.580	−0.233	−0.803	−0.011
82	−0.638	−0.485	−0.152	−0.585	−0.053
83	0.553	0.537	0.016	0.537	0.016
85	−0.808	−0.309	−0.498	−0.809	0.002
86	0.237	0.160	0.076	0.166	0.071
87	0.208	0.556	−0.349	0.256	−0.048
88	0.190	0.506	−0.316	0.309	−0.119
89	−0.121	−0.079	−0.042	−0.287	0.166
90	0.514	0.484	0.030	0.548	−0.034
91	0.215	0.348	−0.134	0.221	−0.006
92	−0.158	−0.033	−0.126	−0.132	−0.026
93	1.097	0.813	0.284	1.254	−0.157
94	0.670	0.624	0.045	0.649	0.021
95	0.162	0.022	0.140	0.309	−0.147
96	0.807	0.624	0.183	0.829	−0.022
97	0.676	0.401	0.274	.406	0.270
98	0.107	−0.073	0.180	−0.086	0.193
99	−0.149	−0.506	0.356	−0.205	0.056
100	−0.517	−0.589	0.072	−0.518	0.001
101	0.136	0.282	−0.146	0.173	−0.037
102	−0.124	0.141	−0.265	0.230	−0.354
104	−0.740	−0.419	−0.321	−0.691	−0.049
105	0.553	0.414	0.139	0.701	−0.148
106	0.013	0.045	−0.032	0.027	−0.014
107	0.893	0.857	0.036	0.726	0.167
109	0.607	0.685	−0.078	0.847	−0.240
110	0.268	0.244	0.023	0.443	−0.175
111	0.721	0.569	0.152	0.619	0.102
112	1.066	0.889	0.176	0.923	0.143
113	0.618	0.426	0.192	0.382	0.236
Test set					
4	1.357	1.375	−0.018	1.283	0.074
7	−1.714	−1.857	0.143	−1.587	−0.127
8	1.770	1.646	0.124	1.724	0.046
11	1.620	1.257	0.363	1.968	−0.348
14	−1.516	−1.045	−0.471	−1.045	−0.471
17	−0.699	−0.689	−0.010	−0.689	−0.010
21	1.523	2.856	−1.333	1.556	−0.033
22	1.699	1.187	0.512	1.387	0.312
30	−0.758	−0.782	0.024	−0.759	0.001
38	1.301	1.338	−0.037	1.305	−0.004
41	1.469	1.378	0.091	1.450	0.019
61	−1.978	−1.326	−0.652	−1.855	−0.123
71	−1.728	−1.420	−0.308	−1.338	−0.390
76	−0.710	0.718	−1.428	0.218	−0.928
84	−1.060	−1.107	0.047	−1.356	0.296
103	−1.072	−1.054	−0.018	−1.033	−0.039
108	0.498	0 .239	0.259	0.509	−0.011

PA = predicted activity, Res. = residual of experimental and predicted activities.

validated with test set of compounds. The squared correlation coefficient (r^2 between EA and PA) value of validation set was 0.958 with standard error of estimation (SEE) 0.287. These results confirm the good prediction ability of this 3D-QSAR model

In the CoMFA model, the steric and electrostatic field contributions are 0.413 and 0.587, respectively. The contour

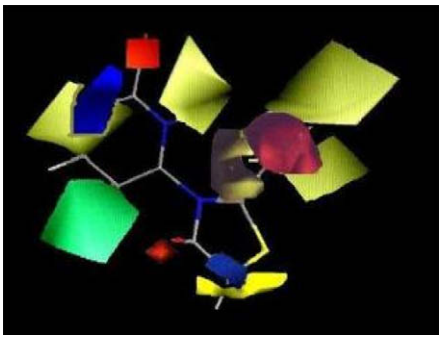

Fig. 3. CoMFA contour maps for steric and electrostatic fields. Green contours indicate regions where bulky groups are favorable for activity, whereas yellow contours indicate regions where bulky groups are not desirable for activity. Blue contours indicate regions where the positive groups could increase activity, whereas red contours indicate the regions needing negative charge.

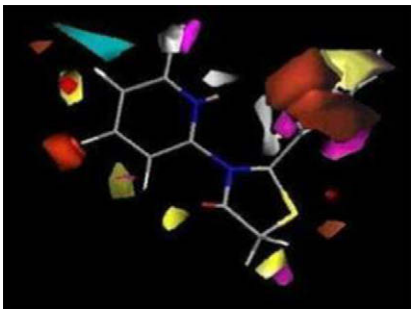

Fig. 4. CoMSIA contour maps for hydrophobic, hydrogen bond acceptor and donor fields. Magenta contours indicate where hydrogen bond acceptor groups are favorable for activity; cyan contours indicate where hydrogen bond donor groups are favorable for activity; red contours indicate where hydrogen bond acceptor groups are not favorable for activity; white contours indicate where hydrophobic groups are favorable for activity and yellow contours indicate where hydrophobic groups are not favorable for activity of thiazolidinones.

maps of this model shown in Fig. 3 illustrate clearly the steric and electrostatic interactions in CoMFA model. In the contour maps electronegative region corresponds to red areas and electropositive region corresponds to blue areas. The red region near the 3′rd substitution position of aromatic ring, and 2″ and 6″th position of another aromatic ring of thiazolidinone derivative suggests that biological activity can be enhanced by introduction of more electronegative groups at this position for strong electrostatic field interactions. The blue region near 4′th position of aromatic ring of thiazolidinone derivative indicates that the biological activity will be decreased by electronegative group at the above-mentioned positions. Yellow contour near the 2′, 4′, 2″, 3″ and 6″th position of aromatic rings of thiazolidinone derivative indicates that the bulky substituents at these positions decrease anti-HIV activity.

The presence of electron withdrawing groups like CN, F, Br, Cl at 3′, 2″ and 6″th position of aromatic ring of thiazolidinone derivative may be conducive to anti-HIV activity. But the same groups if present in 4′th position of ring may be detrimental to activity. The presence of smaller electronegative groups at 2″ and 6″th position of thiazolidinone ring may be conducive to anti-HIV activity.

The contributions of steric, electrostatic, hydrophobic, hydrogen bond acceptor and donor fields in the CoMSIA model are 0.196, 0.360, 0.120, 0.242 and 0.082, respectively. The contour maps of this model shown in Fig. 4 illustrate clearly the hydrophobic, hydrogen bond acceptor and donor field interactions in CoMSIA model. The steric and electrostatic contour map of CoMSIA model is merely same like CoMFA steric and electrostatic contour maps. The white contour near 3′, 2″ and 6″th position of aromatic rings indicates that substitution of hydrophobic groups at these positions is conducive to anti-HIV activity. It indicates that these hydrophobic groups may interact with amino acid residues (Leu234, Tyr318, His235, Phe227, Trp229, Tyr118) of HIV-1 reverse transcriptase and inhibit the HIV multiplication. The yellow contour at 4′, 3″ and 4″th position of aromatic rings suggests that the hydrophobic groups at these regions are not favorable for biological activity. The magenta contour over 3′, 2″ and 6″th position of aromatic rings indicates that hydrogen bond acceptors at these positions are favorable for anti-HIV activity of thiazolidinone derivatives. It indicates that this hydrogen bond acceptor group may be responsible for hydrogen-bonding interaction with amino acid residues (Val179 and Lys101) of HIV-1 reverse transcriptase and may inhibit the HIV multiplication. The cyan contour near 4′th position of aromatic ring indicates that hydrogen bond donor at this position is favorable for anti-HIV activity. Meanwhile the red contour over 2″ and 6″th position of aromatic ring indicates that the presence of hydrogen bond donor groups at these positions are detrimental to anti-HIV activity of thiazolidinone derivatives.

4. Conclusion

A ligand-based approach is used in rational drug design to build activity models which provide important information on possible improvements in ligand structure to increase activity. In the present study, we constructed satisfactory 3D-QSAR models of thiazolidinone derivatives using CoMFA and CoMSIA methods based on the field fit molecular alignment. The CoMFA QSAR model shows that the steric and electrostatic parts contribute equally to the activity. The CoMSIA QSAR model shows that the hydrogen bond acceptor and electrostatic parts contribute maximum to the activity. The contour maps from CoMFA and CoMSIA provide useful insight into designing novel thiazolidinone compounds with increased anti-HIV activity.

In conclusion, our current studies have established a reliable CoMFA and CoMSIA model indicates that 3′, 2″, 6″ substituted aromatic rings of thiazolidinones are important for anti-HIV activity, which can efficiently guide further modification of thiazolidinone analogs.

Acknowledgment

We would like to thank Prof. B. Suresh, Principal, J.S.S. College of Pharmacy, Ooty, TN, India for providing access to the computational resources. One of the authors VR is thankful to AICTE for providing fellowship for this work.

References

[1] R.C. Gallo, S.Z. Salahuddin, M. Popovic, G.M. Shearer, M. Kaplan, B.F. Haynes, T.J. Palker, R. Redfield, J. Oleske, B. Safai, Science 224 (1984) 500–503.

[2] F. Barre-Sinoussi, J.C. Chermann, F. Rey, M.T. Nugeyre, S. Chamaret, J. Gruest, C. Dauguet, C. Axler-Blin, F. Vezinet-Brun, C. Rouzioux, W. Rozenbaum, L. Montagnier, Science 220 (1983) 868–871.

[3] E.D. Clercq, J. Med. Chem. 38 (1995) 2491–2517.

[4] J. Milton, M.J. Slater, A.J. Bird, D. Spinks, G. Scott, C.E. Price, S. Downing, D.V.S. Green, S. Madar, R. Bethell, D.K. Stammers, Bioorg. Med. Chem. Lett. 8 (1998) 2623–2628.

[5] P. Pungpo, S. Hannongbua, J. Mol. Graph. Model. 18 (2000) 581–590.

[6] M.L. Barreca, A. Carotti, A. Chimirri, A.M. Monforte, Bioorg. Med. Chem. 7 (1999) 2283–2292.

[7] P.R.N. Jayatilleke, A.C. Nair, R. Zauhar, W.J. Welsh, J. Med. Chem. 43 (2000) 4446–4451.

[8] S. Kumar, R.R. Jacob, M. Tiwari, Indian J. Pharm. Sci. 67 (2005) 30–36.

[9] R. Garag, D. Patel, Bioorg. Med. Chem. Lett. 15 (2005) 1367–1370.

[10] B. Bhhatarai, R. Garg, Bioorg. Med. Chem. 13 (2005) 4078–4084.

[11] J.K. Buolamwini, H. Assefa, J. Med. Chem. 45 (2002) 841–852.

[12] K. Raghavan, J.K. Buolamwini, M.R. Fesen, Y. Pommier, K.W. Kohn, J. Med. Chem. 38 (1995) 890–897.

[13] A.K. Debnath, S. Jiang, N. Strick, K. Lin, P. Haberfield, J. Med. Chem. 37 (1994) 1099–1108.

[14] J.T. Leonard, K. Roy, Bioorg. Med. Chem. 14 (2006) 1039–1046.

[15] J.T. Leonard, K. Roy, Bioorg. Med. Chem. Lett. 16 (2006) 4467–4474.

[16] K.K. Sahu, V. Ravichandran, V.K. Mourya, R.K. Agrawal, Med. Chem. Res. 15 (2007) 418–430.

[17] K.K. Sahu, V. Ravichandran, P.K. Jain, V.K. Mourya, R.K. Agrawal, Acta Chim. Slov. 55 (2008) 138–145.

[18] V. Ravichandran, R.K. Agrawal, Bioorg. Med. Chem. Lett. 17 (2007) 2197–2202.

[19] V. Ravichandran, V.K. Mourya, R.K. Agrawal, Arkivoc XIV (2007) 204–212.

[20] V. Ravichandran, P.K. Jain, V.K. Mourya, R.K. Agrawal, Med. Chem. Res. 16 (2007) 342–351.

[21] V. Ravichandran, V.K. Mourya, R.K. Agrawal, Internet Electron, J. Mol. Des. 6 (2007) 363–374.

[22] V. Ravichandran, B.R. Prashanthakumar, S. Sankar, R.K. Agrawal, Med. Chem. Res. 17 (2007) 1–11.

[23] V. Ravichandran, V.K. Mourya, R.K. Agrawal, Digest J. Nanomat. Biostruct. 3 (2008) 9–17.

[24] A. Rao, J. Balzarani, A. Carbone, A. Chimirri, E.D. Clercq, A.M. Monforte, P. Monforte, C. Pannecouque, M. Zappala, Antiviral Res. 63 (2004) 79–84.

[25] R.K. Rawal, R. Tripathi, S.B. Katti, C. Pannecouque, E.D. Clercq, Bioorg. Med. Chem. 15 (2007) 3134–3142.

[26] A. Rao, J. Balzarani, A. Carbone, A. Chimirri, E.D. Clercq, A.M. Monforte, P. Monforte, C. Pannecouque, M. Zappala, Farmaco 59 (2004) 33–39.

[27] M.L. Barreca, J. Balzarini, A. Chimirri, E.D. Clercq, L.D. Luca, A.M. Monforte, P. Monforte, C. Pannecouque, A. Rao, M. Zappala, J. Med. Chem. 45 (2002) 5410–5413.

[28] A. Rao, A. Carbone, A. Chimirri, E.D. Clercq, A.M. Monforte, P. Monforte, C. Pannecouque, M. Zappala, Farmaco 57 (2002) 747–751.

[29] A. Rao, A. Carbone, A. Chimirri, E.D. Clercq, A.M. Monforte, P. Monforte, C. Pannecouque, M. Zappala, Farmaco 58 (2003) 115–120.

[30] O.S. Weislow, R. Kiser, D.L. Fine, J. Bader, R.H. Shoemaker, M.R. Boyd, J. Natl. Cancer Inst. 81 (1989) 577–583.

[31] H.F. Chen, Q. Li, X.J. Yao, B.T. Fan, S.G. Yuan, A. Panaye, J.P. Doucet, QSAR Comb. Sci. 22 (2003) 604–613.

[32] H.F. Chen, Q. Li, X.J. Yao, B.T. Fan, S.G. Yuan, A. Panaye, J.P. Doucet, QSAR Comb. Sci. 23 (2004) 36–55.

[33] SYBYL [computer program], Version 6.7., Tripose Associates Inc., St. Louis, MO, USA, 2003.

[34] M. Clark, R.D. Cramer, N.V. Opdenbosch, J. Comput. Chem. 10 (1989) 982–1012.

[35] A. Tropsha, P. Gramatica, V.K. Gombar, QSAR Comb. Sci. 22 (2003) 1–9.

[36] G. Klebe, U. Abraham, T. Mietzner, J. Med. Chem. 37 (1994) 4130–4136.